Sequential Segmentation of the Left Atrium and Atrial Scars Using a Multi-scale Weight Sharing Network and Boundary-Based Processing

Abbas Khan[1,2], Omnia Alwazzan[1,2], Martin Benning[2,3], and Greg Slabaugh[1,2(✉)]

[1] School of Electronic Engineering and Computer Science, Queen Mary University of London, London, UK
{a.rayabatkhan,g.slabaugh}@qmul.ac.uk
[2] Queen Mary's Digital Environment Research Institute (DERI), London, UK
[3] School of Mathematical Sciences, Queen Mary University of London, London, UK

Abstract. Left atrial (LA) segmentation and quantification of atrial scars have opened a path to automating Atrial Fibrillation (AF) diagnosis. This paper proposes a two-stage approach for sequential segmentation of the LA cavity and scars. Our Multi-scale Weight Sharing (MSWS) Network extracts features at multiple scales and is used for LA cavity segmentation. We also propose a Boundary2Patches method which performs segmentation of scars around the detected LA cavity boundary. The MSWS network learns a better representation of features through sharing weights across scales, and the Boundary2Patches method focuses on smaller scars constrained in the region around the LA cavity wall. On the challenge cohort (validation set), our method achieves an average Dice score of 0.938 and 0.558 for the LA cavity and scars segmentation of task 1, and a Dice score of 0.846 for LA cavity segmentation of task 2. The pre-trained models, source code, and implementation details are available at https://github.com/kabbas570/LAScarQS2022.

Keywords: Left Atrial segmentation · Scar quantification · Atrial fibrillation (AF) · Multi-scale Weight Sharing Network · Boundary2patches

1 Introduction

Atrial Fibrillation (AF) is a condition that produces an irregular, fast or sluggish heartbeat in the upper chamber of the heart. According to the US Centers for Disease Control and Prevention (CDC) [5], AF is one of the most prevalent forms of cardiac arrhythmia that increases the risk of ischemic stroke. Strokes resulting from AF complications are typically more severe than strokes due to other underlying causes [6]. Treatment and diagnosis of AF remain a concern. The assessment of AF patients may depend on the position and size of scars

X. Zhuang et al. (Eds.): LAScarQS 2022, LNCS 13586, pp. 69–82, 2023.
https://doi.org/10.1007/978-3-031-31778-1_7

which could provide vital information about the onset of AF. Late gadolinium enhancement magnetic resonance imaging (LGE MRI) has evolved to assess the extent of scars and the Left Atrial (LA) cavity [10]. The LGE MRI has allowed scientists to automate the time-consuming diagnosis of AF. However, such automation requires LA cavity segmentation and scars quantification.

Analyzing the LGE MRI scans could provide valuable insight for AF diagnosis and treatment stratification [18]; however, the manual delineation of LA scarring and cavities for quantification is laborious and highly subjective [16]; therefore, it is desirable to automate the process. This challenge has attracted considerable research interest even before the era of deep learning. Intensity-based thresholding [12], clustering methods [7], and graph-cuts [17] were popular traditional methods. However, these methods have limitations of computational costs and manual selection for the areas of interest to be segmented.

With the advent of deep learning, LA segmentation and scars quantification have attracted additional research. Several fully automated methods have been proposed in this field. One of the most recent methods by Li et al. [15] utilized shape attention (SA) through a surface projection of the LA cavity and achieved higher performance for scar quantification. The authors used the inherent correlation between the LA cavity and scars, and trained a joint segmentation architecture. A hybrid method based on graph cuts and CNNs was used by [13] for the automatic scar segmentation. A multi-scale three-stage network was used to learn both local and global features. Vesal et al. [20] employed a UNet [19] based model with dilated convolutions in the bottleneck to segment 3D volumetric scans. Each volume is centre-cropped to remove over-represented backgrounds and to learn only a particular region of interest to improve LA segmentation. Bian et al. [3] used a pyramid pooling module to extract the features at different scales and improved the robustness of the model against various shapes of the LA. They also implemented an Online Hard Negative Example Mining strategy to classify a voxel with low certainty. A contour loss is introduced by [9] to provide spatial distance information during training and used in a two-stage, three-dimensional UNet-based architecture. The first UNet generates coarse segmentation maps, and the second UNet refines coarse predictions to segment the LA at a higher resolution accurately. Yang et al. [21] used an atlas-based method to identify the LA cavity first and then used a super-pixel-based approach to detect the scars in that region. Campello et al. [4] introduced a CyclicGan to first increase the number of annotated LGE MRI scans followed by a modified UNet [19] network to perform scar tissue segmentation.

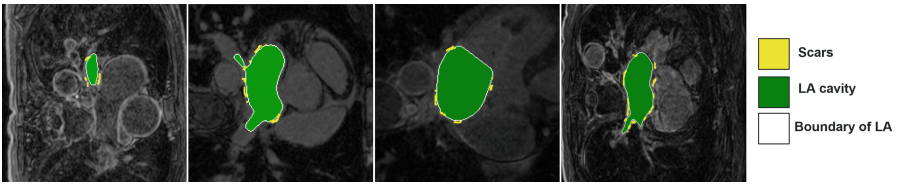

Fig. 1. Visualisation of LA cavity and scars from LAScarQS 2022 challenge dataset.

Challenges remain however, mostly because of the poor quality of annotated LGE MRI scans, the heterogeneity of LA shape and appearance, and the presence of small scars and thin tissue walls. Accordingly, the LAScarQS 2022 competition [14–16] seeks a solution to the aforementioned problems by focusing on the LA cavity and scars segmentation from LGE MRI. For illustration, Fig. 1 shows examples of LGE MRIs scan from the LAScarQS 2022 challenge dataset.
In this paper, we focus on segmenting the LGE MRI scans over multiple scales by concurrently sharing the weights and enabling the kernels to learn shared representations of features using MSWS-Net. In a second stage, we propose a Boundary2Patches method to detect the scars around the LA boundary and quantify the scars using patches and a modified UNet architecture.

2 Proposed Approach

Fig. 2 presents the proposed sequential segmentation framework, for both the LA cavity and scars segmentation. First, we segment the LA cavity using MSWS-Net and then use its output as an initialization step for scar quantification. In Fig. 2, the black arrows represent the workflow for LA cavity segmentation, the lime green arrows for scars segmentation (Boundary2Patches method), and the orange color is used only for visualisation, i.e. it is not part of training or inference. For both tasks, the training is performed separately; but the two steps are merged together during inference in an sequential manner. The following subsections will explain in detail each network and the post-processing steps adopted during training and testing.

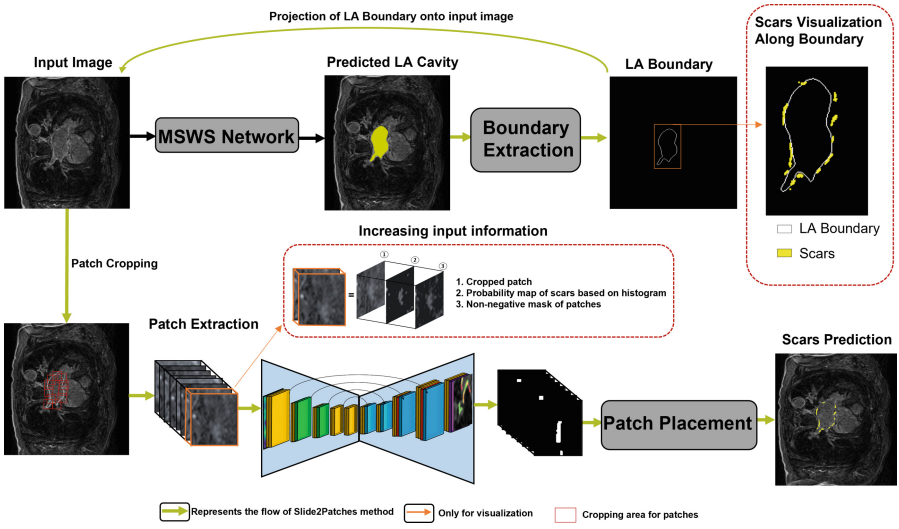

Fig. 2. A schematic of the proposed sequential approach for LA and atrial scars segmentation.

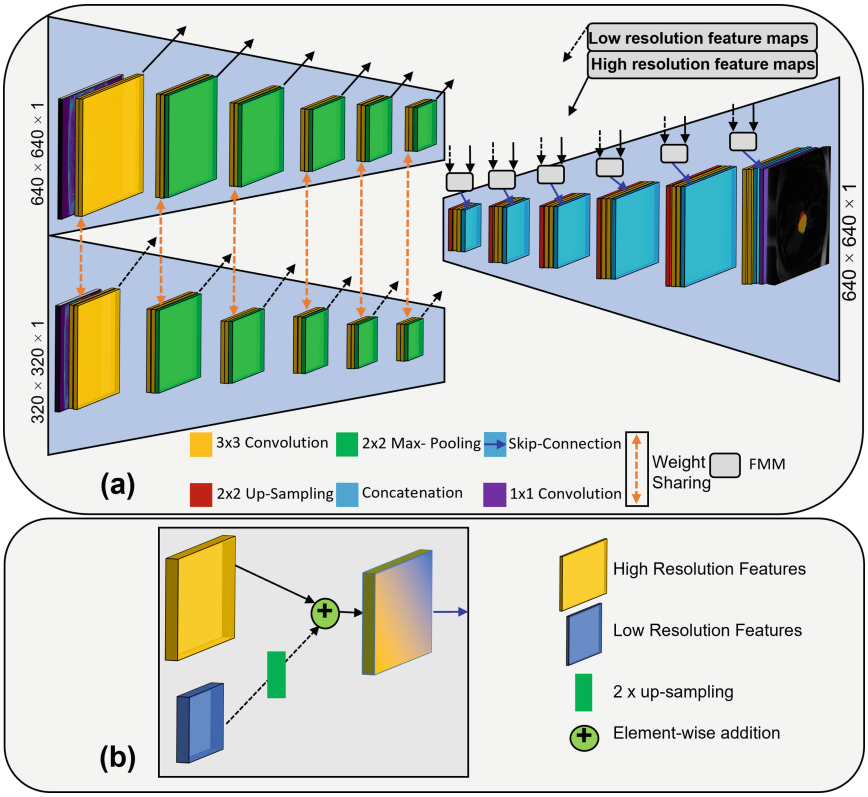

Fig. 3. The proposed Multi-Scale Weight Sharing Network. (a) Extracting features at various scales from the input. (b) The feature merging module; combining low and high resolution features.

2.1 Multi-Scale Weight Sharing Network (MSWS-Net)

In this paper, we propose the concept of weight sharing over several scales, namely, Multi-scale Weight Sharing Network (MSWS-Net), as illustrated in Fig. 3. All the weight sharing stages must have the same number of kernels in each layer. In a conventional encoder-decoder architecture such as UNet, the features are extracted from only a single scale of input and down-sampled by multiple factors; thus, the convolutional kernels only learn a single scale features from the input space. Instead, we employ the concept of kernel sharing across several scales and make kernels capable of learning the same characteristics from various input spaces. Furthermore, all kernels share the same parameters at each encoder stage; thus, the overall number of parameters in the architecture does not increase, and the network benefits from convolving the same kernels with varying dimensions of incoming feature maps. We experimented with different numbers of encoders $n \in [2, 4]$ and discovered that n = 2 performed best while $n > 2$ did not improve the results significantly, detailed experiments are men-

tioned in Table 1. We speculate that the LA cavity appears self-similar at these two scales, and increasing the number of encoders beyond 2 has no effect on the network's learning ability. Therefore, in our final implementation, we set n = 2. The optimal number of multi-scale levels depends upon the dataset's self-similarity across scale, and a performance boost may vary for different datasets.

The proposed multi-scale weight sharing (MSWS) architecture is depicted in Fig. 3. It takes two images as input with dimensions [H x W x C] and [H/2 x W/2 x C]; note that number of channels should be the same for both images. For this challenge, we resized all images to H = 640 and W = 640 using zero padding. Furthermore, each 2D scan was normalized to zero mean and unit variance. Two consecutive 3×3 convolutions are performed at each encoder stage, followed by ReLU activation and batch-normalization. The proposed weight-sharing strategy across multiple scales will help the network to learn the features of different scales. The shared weights are represented by an orange vertical dotted arrow. At the decoder side, the features of various scales are combined using a feature merging module (FMM) at each stage. The FMM merges the information across two-resolution representations. First, it upsamples the lower resolution features with a factor = 2, and then it preforms an element-wise addition with the corresponding incoming features from the other encoder. The resultant representation is semantically richer and spatially more precise; helping to segment various shapes of LA cavity efficiently. In Fig. 3, the black arrow, dotted black arrow and blue arrow represents features of higher-resolution, lower-resolution, and merged features, respectively.

2.2 Boundary Processing with the Boundary2Patches Method

Fig. 2 depicts a broad overview of the proposed boundary-based processing method, namely, Boundary2Patches for the scars segmentation. As previously indicated, the proportion of scars is relatively small compared to the entire image; therefore, we restricted the search area using the Boundary2Patches approach to concentrate more on the scars. Current literature implies that scars are most prevalent across the LA cavity's boundary; hence, we solely search for scars in the region adjacent to the LA wall. From the LA cavity segmentation, the boundary of the LA cavity is identified and 64×64 patches from the original image are extracted along the boundary, as illustrated in Fig. 2. The patch size of 64×64 is selected as it incorporates all the surrounding scars if we reconstruct the ground truth from these patches. For Boundary2Patches method, we trained another encoder-decoder network separately and ran it sequentially with MSWS-Net during inference. The architecture used for Boundary2Patches method is shown in Fig. 4. It has four stages (two consecutive 3×3 convolutions at each stage with ReLU activation and batch-normalization) at the respective encoder and decoder sides. For the encoder, features are down-sampled twice using strided convolution with stride = 2 to avoid the loss of information for small-size scars. On the decoder side, transposed convolutions are used to upsampled the incoming features, and the upsampled features are concatenated with corresponding

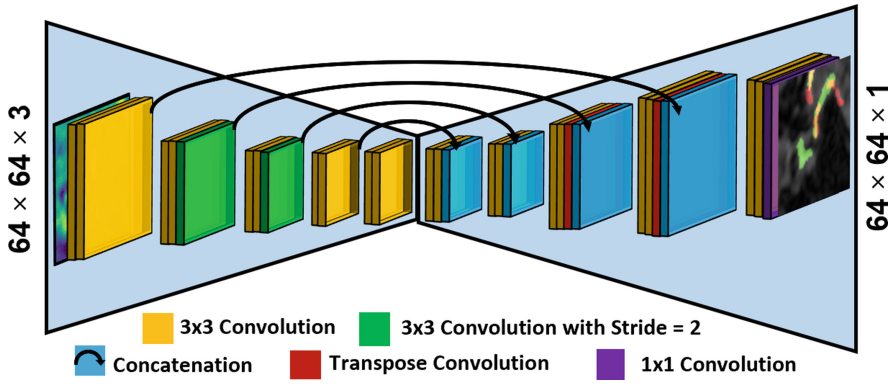

Fig. 4. The modified UNet architecture for scars segmentation.

features of the encoder for better gradient flow. Sigmoid was used as an activation function for the last output layer with 1×1 convolution to generate the segmentation map for scars.

In the final implementation, we further increased the input information by concatenating the patches with a probability map of scar based on histogram and non-negative values obtained after z-score normalization. We discovered that in LGE MRI, scars have greater intensities than the surrounding areas, thus we computed the histogram of higher intensities and used it in conjunction with extracted patches and a non-negative mask of scars, as illustrated in Fig. 2.

3 Dataset Description

The dataset was provided by the LAScarQS 2022 Challenge, which intends to develop automated/semi-automated methods for segmenting the LA Multi-Center LGE MRIs and quantifying scars. The dataset consists of 194 LGE MRIs. The MRI scans of LGE were produced at two distinct locations using scanners with varying resolutions. The included gold standard labels consist of the LA blood pool (atriumSegImgMO.nii.gz) as well as the LA scars (scarSegImgM.nii.gz). Furthermore, training and testing on the dataset can be conducted remotely from several local centers while the dataset remains concealed to preserve data privacy. During the training phase, the dataset was subdivided into 70% for training, 20% for validation, and 10% for inference to evaluate our proposed models and undertake ablation experiments.

4 Experimental Details

The proposed framework was implemented in PyTorch, and all the experiments were performed using a cluster of NVidia A100 GPUs [1]. For both approaches,

MSWS-Net and Boundary2Patches, the models were trained using Adam optimization [11], with β_1, β_2= [0.9,0.99], and the learning rate was set to = 0.0001. During training, we set the maximum number of epochs to 100 and the batch size to 24. In addition, we employed a custom early stopping mechanism from terminating the training before the model overfits the data. In our customized early stopping method, we monitored the validation loss and Dice score and halted training if either was not improving for five consecutive epochs.

4.1 Loss Function

While analyzing the data, we found that the LA cavity and scars occupy a small fraction of the full image. Such imbalance in the data could not be handled by commonly used loss functions for segmentation, such as the Dice loss or binary cross entropy loss, as listed in Table 2. Initially, MSWS-Net was trained with a weighted Dice loss, but this led to a greater number of false negatives (FNs) than false positives (FPs). Consequently, we trained both networks with the Focal Tversky loss function [2] given by Eqs. 1 and 2,

$$TI_c = \frac{\sum_{i=1}^{N} \hat{y}_{ic} y_{ic} + \epsilon}{\sum_{i=1}^{N} \hat{y}_{ic} y_{ic} + \beta \sum_{i=1}^{N} (1 - \hat{y}_{i\bar{c}}) y_{ic} + \alpha \sum_{i=1}^{N} \hat{y}_{ic} (1 - y_{i\bar{c}}) + \epsilon} \tag{1}$$

$$FTL_c = \sum_{c} (1 - TI_c)^{1/\gamma} \tag{2}$$

where $\hat{y}_{ic}$ is the probability that the pixel is from the LA cavity and y_{ic} is the probability of background class. The hyperparameter α focuses on FPs, β focuses on FNs, and γ focuses on hard examples. These hyperparameters are tuned to get a balance between precision and recall in the case of large class imbalance. In our experiments, we trained MSWS-Net with α, β, γ = [0.3,0.7,0.75] and the Boundary2Patches method with α, β, γ = [0.4,0.6,0.75].

5 Results and Discussion

This section describes the results of our methods applied to the validation data for Tasks 1 and 2 of the LAScarQS 2022 challenge. In addition, we performed ablation studies to measure the effectiveness of the proposed methods. Finally, MSWS-Net is compared to two of its ablated variants, while Boundary2Patches was compared to two baseline schemes. The following list overviews four experiments conducted in this paper.

1. **Standard UNet Architecture:** The ability of proposed MSWS-Net to extract features at multiple-scales is compared to a standard UNet architecture with a single encoder and the same number of stages as MSWS-Net.

2. **MSWS-Net without weight sharing:** The weight sharing strategy is evaluated by training the MSWS-Net without sharing the weights of two encoders.

3. **Center-Cropping:** We trained the network depicted in Fig. 4 on centred cropped images for scar quantification and compared the results with the patch-based technique.

4. **Without using the increased input information:** We solely used the cropped patches in the Boundary2Patches method to evaluate the benefit of employing the additional information concatenated at the input of the network.

5. **Choice of Loss function:** We experimented with various loss functions and their combinations. Due to the small volume of the to-be-segmented region of interest, we modified the focal loss using Tversky loss to reduce the number of false negatives and achieve the optimal tradeoff between precision and recall. Table 2 summarizes the results of various loss functions.

6. **Number of Weight-Sharing Encoders for MSWS-Net:** For MSWS-Net, we increased the number of encoders from 1 to 4 while sharing the weights and having spatial dimensions in the range of H × W to $\frac{H}{2^n} \times \frac{W}{2^n}$, where 'n' is the number of encoders. We found that n = 2 is the optimal tradeoff between performance and network complexity for the task at hand. By increasing the 'n', the performance gain was statistically insignificant at the expense of slower processing and requiring more resources. Table 1 shows the results of ablation studies conducted to choose optimal number of Weight-Sharing Encoders for MSWS-Net.

Table 1. Ablation studies to choose optimal number of weight sharing encoders, Giga Floating Point Operations per Second (GFLOPs), Input Size, and Dice score.

# of Encoders	GFLOPs ↓	Input Size (MB) ↓	Dice Score ↑
1	**310.80**	**1.56**	0.828
2	339.31	1.95	0.918
3	346.44	2.05	0.920
4	348.22	2.10	**0.922**

Table 2. Comparison of different loss functions on validations set of task: 1. TPs: True Positives, FPs: False Positives, FNs: False Negatives, IoU: Intersection over Union.

Loss Function	Dice Score ↑	TPs ↑	FPs ↓	FNs ↓
Binary-Cross Entropy	0.895	1,821,410	112,551	305,740
1-IoU	0.906	1,857,001	106,154	270,149
Focal Tversky	**0.918**	**1,847,210**	**109,765**	**136,254**

5.1 LA Cavity Segmentation: Task 2

For this task, MSWS-Net is able to segment the LA cavity of different shapes accurately, achieving a Dice score of 0.846 on the validation set. Table 3 shows the results of the aforementioned ablation experiments and demonstrates the effectiveness of multiple scale encoders and weight-sharing schemes. Different evaluation metrics such as Dice score (DS), Hausdorff Distance (HD), average surface distance (ASD), and sensitivity were used to quantify the segmentation performance. The qualitative results are shown in Fig. 5, comparing the visual performance of MSWS-Net with its ablated versions. The third row indicates the results of MSWS-Net, whereas the first and second rows represent the results of standard UNet and MSWS-Net without the weight sharing approach.
For visualization purposes, we have projected the ground truth and predicted segmentation maps on the input images. In addition, we have assigned different colors to all qualitative results reported in this paper (Green represents false positives, Red represents false negatives, and Yellow represents true positives).

5.2 LA Cavity and Scars Segmentation: Task 1

Task 1 of the challenge aims to segment the LA cavity and the atrial scars. For scar quantification, we first segmented the LA cavity and then used the Boundary2Patches approach to find scars along the LA boundary, where they are predominantly present. The performance of the scar segmentation relies on the precise segmentation of the LA cavity. To improve the segmentation of the LA cavity, we first trained the MSWS-Net on training data from Task 2 and then fine-tuned it on Task 1. Ultimately, we obtained a Dice score of 0.938 for the LA cavity segmentation of Task 1 on the validation set. Figure 6 presents qualitative results for LA cavity segmentation from Task 1 of the challenge.

For scar quantification, we used the boundaries of predicted LA cavities, which are predicted via MSWS-Net, to crop the patches during the inference stage. The number of cropped patches during inference differed for each image, depending upon the area of the segmented LA cavity. Table 4 summarizes the performance of the proposed Boundary2Patches method for scar segmentation. For comparison purposes, we centred cropped the images (384×384) and tried to predict the scars, which resulted in lower performance, as listed in Table 4. We also highlighted the importance of using the increased input information at

Table 3. Validation dataset benchmarks quantitative results for Task 2 of LA cavity segmentation and comparison of MSWS-Net with its ablated versions.

Method	Dice Score ↑	HD (mm) ↓	ASD (mm) ↓
Standard UNet architecture	0.728	**96.5**	**3.22**
MSWS-Net without weight sharing	0.708	107.2	5.6
MSWS-Net	**0.846**	105.7	3.39

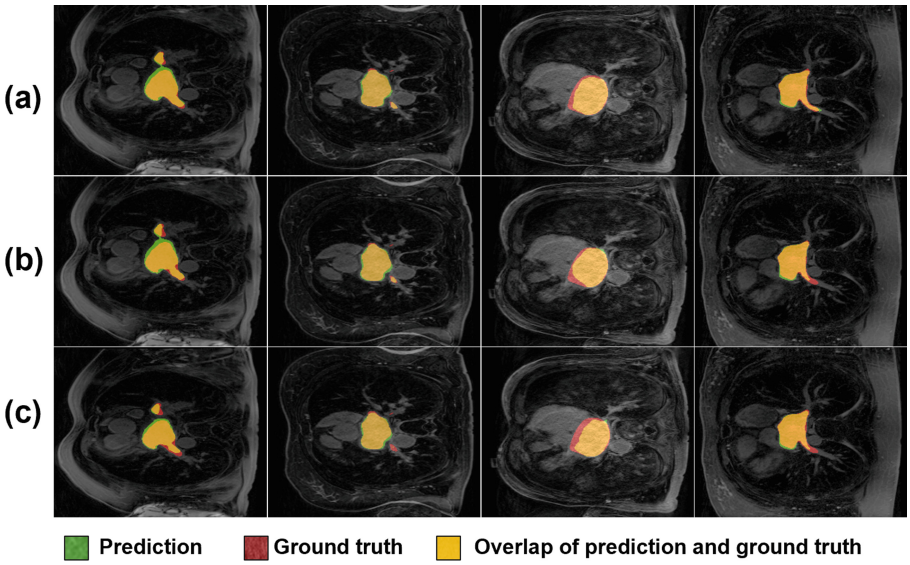

Fig. 5. Qualitative results for Task 2 (LA cavity segmentation). Results of (a) proposed MSWS-Net (b) Standard UNet architecture (c) MSW-Net without weight sharing strategy.

the input of our network by comparing it to an ablated version of the Boundary2Patches method without the additional input derived from the histogram and non-negative mask. Some visual results of scar quantification are shown in Fig. 7.

We additionally applied the connected component analysis (CCA) [8] as a post-processing step on scar segmentation maps to eliminate small false positives from the final predictions, which resulted in a boost of 1.06% in the Dice score for scar quantification, as listed in Table 4. For the CCA implementation, we used the 4-connected component method and discarded components with less than 10 pixels or more than 450. These numbers were chosen empirically. The CCA algorithm also reduced the detection of true positives, but their dismissal ratio was

Table 4. Validation dataset benchmarks quantitative results for scars quantification and comparison of different ablation studies for the Boundary2Patches method.

Method	Dice Score ↑	Sensitivity ↑
Center-Cropping	0.407	0.412
Boundary2Patches (single channel input)	0.465	0.484
Boundary2Patches (three channel input)	0.547	0.559
Boundary2Patches (three channel input + post-processing with CCA)	**0.558**	**0.568**

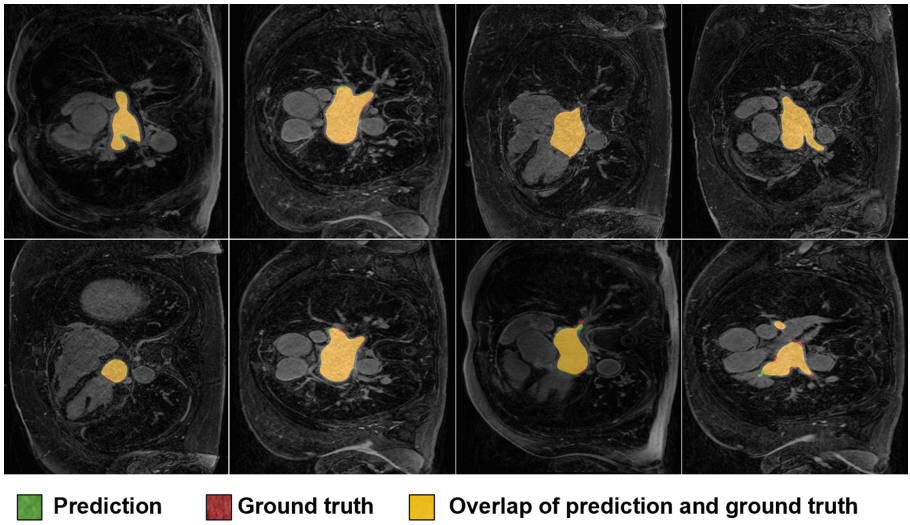

Fig. 6. Qualitative results for Task 1 of LA cavity segmentation.

far less than the removal of false positives, which resulted in improved performance. Figure 8 showcases the visual motivation of applying the CCA technique. It helped to remove the false positive outliers highlighted through the yellow dotted box.

Furthermore, the segmentation performance of the proposed MSWS-Net and Boundary2Patches method in the LAScarQS 2022 testing set is reported in Table 5. For task-1, the test set comprises 22 images, and for task-2, it has

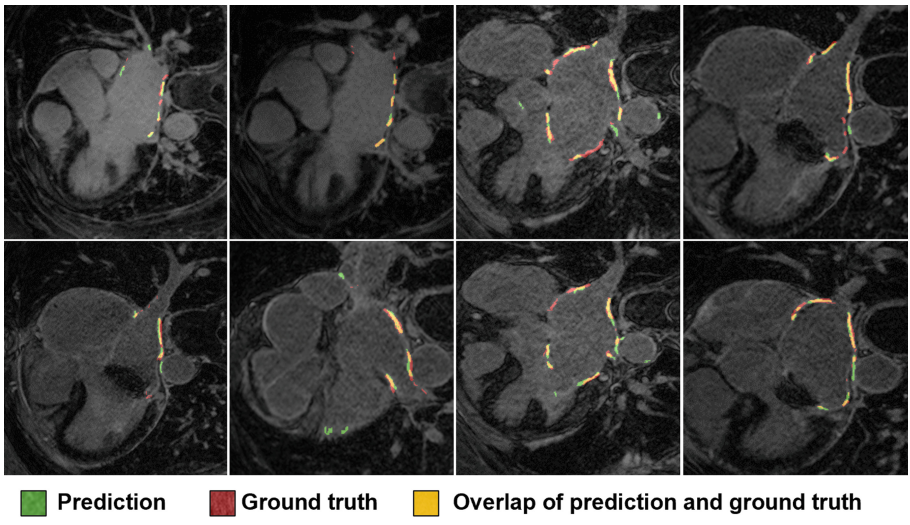

Fig. 7. Visual results for scar quantification of Task 1.

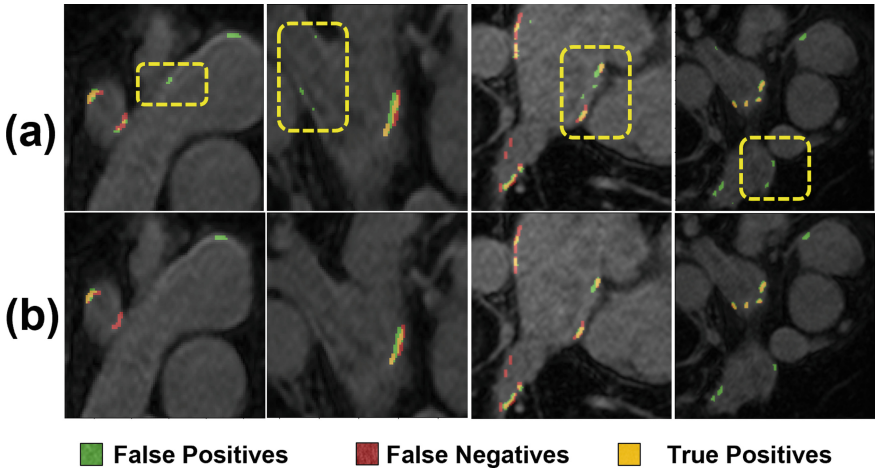

Fig. 8. Removal of small size false positive predictions through CCA technique. (a) Predictions before applying CCA (b) Refined predictions after applying CCA.

44. We observed that the overall performance on the test set is very similar to those of the validation benchmarks. For the test phase, the challenge required a docker file submission. The results are reported in terms of Dice score, HD, and ASD for LA cavity segmentation and for scars quantification; we evaluated the performance using Dice score and sensitivity metrics.

Table 5. LAScarQS 2022 testing dataset benchmarks quantitative results for LA cavity segmentation and scars quantification.

Task	Dice Score ↑	HD (mm) ↓	ASD (mm) ↓	Sensitivity ↑
Task-1 LA cavity segmentation	0.922	110.65	3.48	-
Task-2 LA cavity segmentation	0.792	67.45	2.89	-
Task-1 scars quantification	0.549	-	-	0.599

6 Conclusion

For the LAScarQS 2022 challenge, we propose a sequential approach to segment left atrium and atrial scars using a multi-scale weight-sharing network and boundary-based processing. As the challenge seeks to resolve two problems jointly, namely the LA cavity's segmentation and the quantification of scars, we divided into two sub-tasks to address them together. Essentially, the MSWS-Net extracts features at various scales, and learns a more accurate representation of features via multi-scaling and weight-sharing techniques. Additionally, the

Boundary2Patches method aids in focusing on and accurately segmenting small scars. Lastly, the proposed approach achieves an average Dice score of 0.938 and a Dice score of 0.558 for the segmentation of LA cavities and scars, respectively, in Task 1, as well as an average Dice score of 0.846 for the segmentation of LA cavities in Task 2.

Acknowledgements. This research work is funded by the mini-Centre for Doctoral Training (CDT) award through the Faculty of Science and Engineering, Queen Mary University of London, United Kingdom. The authors also thank project partners, including NVIDIA Corporation, Circle Cardiovascular Imaging, and Conavi Medical.

References

1. This research utilised queen mary's andrena HPC facility, supported by QMUL research-it. https://zenodo.org/record/438045 Accessed 20 May 2022
2. Abraham, N., Khan, N.M.: A novel focal Tversky loss function with improved attention u-net for lesion segmentation. In: 2019 IEEE 16th International Symposium on Biomedical Imaging (ISBI 2019), pp. 683–687. IEEE (2019)
3. Bian, C., et al.: Pyramid Network with Online Hard Example Mining for Accurate Left Atrium Segmentation. In: Pop, M., et al. (eds.) STACOM 2018. LNCS, vol. 11395, pp. 237–245. Springer, Cham (2019). https://doi.org/10.1007/978-3-030-12029-0_26
4. Campello, V.M., Martín-Isla, C., Izquierdo, C., Petersen, S.E., Ballester, M.A.G., Lekadir, K.: Combining Multi-Sequence and Synthetic Images for Improved Segmentation of Late Gadolinium Enhancement Cardiac MRI. In: Pop, M., et al. (eds.) STACOM 2019. LNCS, vol. 12009, pp. 290–299. Springer, Cham (2020). https://doi.org/10.1007/978-3-030-39074-7_31
5. Centers for Disease Control and Prevention CDC: centers for disease control and prevention CDC, Atrial Fibrillation (2017). https://www.cdc.gov/heartdisease/atrial_fibrillation.htm Accessed 12 July 2022
6. Chugh, S.S., et al.: Worldwide epidemiology of atrial fibrillation: a global burden of disease 2010 study. Circulation **129**(8), 837–847 (2014)
7. Detsky, J.S., Paul, G., Dick, A.J., Wright, G.A.: Reproducible classification of infarct heterogeneity using fuzzy clustering on multi contrast delayed enhancement magnetic resonance images. IEEE Trans. Med. Imaging **28**(10), 1606–1614 (2009)
8. Fu, Y., Chen, X., Gao, H.: A new connected component analysis algorithm based on max-tree. In: 2009 8TH IEEE International Conference on Dependable, Autonomic and Secure Computing, pp. 843–844 IEEE (2009)
9. Jia, S., et al.: Automatically Segmenting the Left Atrium from Cardiac Images Using Successive 3D U-Nets and a Contour Loss. In: Pop, M., et al. (eds.) STACOM 2018. LNCS, vol. 11395, pp. 221–229. Springer, Cham (2019). https://doi.org/10.1007/978-3-030-12029-0_24
10. Kim, R.J., et al.: Relationship of MRI delayed contrast enhancement to irreversible injury, infarct age, and contractile function. Circulation **100**(19), 1992–2002 (1999)
11. Kingma, D.P., Ba, J.: Adam: a method for stochastic optimization (2014) arXiv preprint arXiv:1412.6980
12. Kolipaka, A., Chatzimavroudis, G.P., White, R.D., O'Donnell, T.P., Setser, R.M.: Segmentation of non-viable myocardium in delayed enhancement magnetic resonance images. Int. J. Cardiovasc. Imaging **21**(2), 303–311 (2005)

13. Li, L., et al.: Atrial Scar Segmentation via Potential Learning in the Graph-Cut Framework. In: Pop, M., et al. (eds.) STACOM 2018. LNCS, vol. 11395, pp. 152–160. Springer, Cham (2019). https://doi.org/10.1007/978-3-030-12029-0_17
14. Li, L., Zimmer, V.A., Schnabel, J.A., Zhuang, X.: Atrial General: domain generalization for left atrial segmentation of multi-center LGE MRIs. In: de Bruijne, M., et al. (eds.) MICCAI 2021. LNCS, vol. 12906, pp. 557–566. Springer, Cham (2021). https://doi.org/10.1007/978-3-030-87231-1_54
15. Li, L., Zimmer, V.A., Schnabel, J.A., Zhuang, X.: Atrialjsqnet: a new framework for joint segmentation and quantification of left atrium and scars incorporating spatial and shape information. Med. Image Anal. **76**, 102303 (2022)
16. Li, L., Zimmer, V.A., Schnabel, J.A., Zhuang, X.: Medical image analysis on left atrial LGE MRI for atrial fibrillation studies: A review. Med. Image Anal., p. 102360 (2022)
17. Lu, Y., Yang, Y., Connelly, K.A., Wright, G.A., Radau, P.E.: Automated quantification of myocardial infarction using graph cuts on contrast delayed enhanced magnetic resonance images. Quant. Imaging Med. Surg. **2**(2), 81 (2012)
18. Njoku, A., et al.: Left atrial volume predicts atrial fibrillation recurrence after radiofrequency ablation: a meta-analysis. Ep Europace **20**(1), 33–42 (2018)
19. Ronneberger, O., Fischer, P., Brox, T.: U-Net: Convolutional Networks for Biomedical Image Segmentation. In: Navab, N., Hornegger, J., Wells, W.M., Frangi, A.F. (eds.) MICCAI 2015. LNCS, vol. 9351, pp. 234–241. Springer, Cham (2015). https://doi.org/10.1007/978-3-319-24574-4_28
20. Vesal, S., Ravikumar, N., Maier, A.: Dilated Convolutions in Neural Networks for Left Atrial Segmentation in 3D Gadolinium Enhanced-MRI. In: Pop, M., et al. (eds.) STACOM 2018. LNCS, vol. 11395, pp. 319–328. Springer, Cham (2019). https://doi.org/10.1007/978-3-030-12029-0_35
21. Yang, G., et al.: Fully automatic segmentation and objective assessment of atrial scars for long-standing persistent atrial fibrillation patients using late gadolinium-enhanced mri. Med. Phys. **45**(4), 1562–1576 (2018)